

PARTON DISTRIBUTIONS IN NUCLEI AT SMALL X

INA SARCEVIC

*Department of Physics, University of Arizona, Tucson, AZ 85721, USA
E-mail: ina@gluon.physics.arizona.edu*

We study the nuclear shadowing effect in the context of Glauber-Gribov multiple-scattering model and perturbative QCD. We find that at small x , the Q^2 evolution of the shadowing is much slower than the DGLAP evolution, due to the multiple scatterings at small x . We show that the gluon shadowing at small x and for $Q^2 > 3\text{GeV}^2$ is perturbative in nature and does not depend on the initial, non-perturbative condition. We evaluate the impact parameter dependence of the gluon distribution and show that it is a non-linear effect in the nuclear thickness function.

The semihard processes, such as minijets, dileptons, open charm and direct photon production in heavy-ion collisions at $\sqrt{s} \geq 200 \text{ GeV}$, can be reliably calculated in the framework of perturbative QCD assuming the validity of the factorization theorem in perturbation theory, and with the knowledge of parton distributions in nuclei at small x .

Quark distribution in nuclei has been measured and the attenuation has been firmly established experimentally at CERN ¹ and Fermilab ² in the region of small x in deeply-inelastic lepton scatterings (DIS) off nuclei. The data, taken over a wide kinematic range, $10^{-5} < x < 0.1$ and $0.05 \text{ GeV}^2 < Q^2 < 100 \text{ GeV}^2$, show a systematic reduction of nuclear structure function $F_2^A(x, Q^2)/A$ with respect to the free nucleon structure function $F_2^N(x, Q^2)$. However, there is no experimental measurement of the gluon density in nuclei.

At low Q^2 , in DIS, the interaction of the virtual photon with the nucleons in the rest frame of the target is most naturally described by a vector-meson-dominance (VMD) model ³. At $Q^2 > 1 \sim 2 \text{ GeV}^2$, the virtual photon can penetrate the nucleon and probe the partonic degrees of freedom where a partonic interpretation based on perturbative QCD is most relevant in the infinite momentum frame. In the target rest frame, the virtual photon interacts with nucleons via its quark-antiquark pair ($q\bar{q}$) color-singlet fluctuation ⁴. If the coherence length of the virtual photon is larger than the distance between nucleons in a nucleus, $l_c > R_{NN}$, the $q\bar{q}$ configuration interacts coherently with fraction of the nucleons, while for $l_c > R_A$ (i.e. $x < 10^{-2}$), it interacts coherently with all the nucleons, with a cross section given by the color transparency mechanism for a point-like color-singlet configuration, $\sigma_{q\bar{q}N} = \frac{4\pi^2}{3} r_t^2 \alpha_s x' g_{\text{DLA}}(x', 1/r_t^2)$ ⁶. This results in a reduction of the total cross section and consequently attenuation of the parton distributions in nu-

clei.

In the Glauber-Gribov multiple-scattering theory⁵ nuclear collision is a succession of collisions of the probe with individual nucleons within nucleus. A partonic system (h), being a $q\bar{q}$ or a gg fluctuation, can scatter coherently from several or all nucleons during its passage through the target nucleus. The interference between the multiple scattering amplitudes causes a reduction of the hA cross section compared to the naive scaling result of A times the respective hN cross section, the origin of the nuclear shadowing. The total hA cross section is given by

$$\sigma_{hA} = \int d^2\mathbf{b} 2 \left[1 - e^{-\sigma_{hN} T_A(\mathbf{b})/2} \right] = 2\pi R_A^2 [\gamma + \ln \kappa_h + E_1(\kappa_h)] , \quad (1)$$

where $\kappa_h = A\sigma_{hN}/(2\pi R_A^2)$ is an impact parameter averaged effective number of scatterings. For small value of κ_h , $\sigma_{hA} \rightarrow 2\pi R_A^2 \kappa_h = A\sigma_{hN}$, the total hA cross section is proportional to A . In the limit $\kappa_h \rightarrow \infty$, the destructive interference between multiple scattering amplitudes reduces the cross section, $\sigma_{hA} \rightarrow 2\pi R_A^2 (\gamma + \ln \kappa_h)$. Namely, the effective number of scatterings is large and the total cross section approaches the geometric limit $2\pi R_A^2$, a surface term which varies roughly as $A^{2/3}$.

In the Glauber-Gribov eikonal approximation,

$$\sigma(\gamma^* A) = \int d^2 b \int_0^1 dz \int d^2 \mathbf{r} |\psi(z, \mathbf{r})|^2 2(1 - e^{-\sigma_{q\bar{q}N}(\mathbf{r}, z) T_A(b)/2}), \quad (2)$$

where $|\psi(z, \mathbf{r})|$ is the photon wave function⁷ and z is the fraction of the energy carried by the quark (antiquark). The nuclear cross section is therefore reduced when compared to the simple addition of free nucleon cross sections.

At small x , the structure function of a nucleus, $F_2^A(x, Q^2)$ can be obtained from $\sigma(\gamma^* A)$. Substituting integration over (z, \mathbf{r}_t) to (x', Q'^2) in (2), one obtains for (sea)quarks⁸

$$xf_A(x, Q^2) = xf_A(x, Q_0^2) + \frac{3R_A^2 x}{8\pi^2} \int_x^1 \frac{dx'}{x'^2} \int_{Q_0^2}^{Q^2} dQ'^2 [\gamma + \ln(\kappa_q) + E_1(\kappa_q)] \quad (3)$$

where $\kappa_q(x, Q^2) = \frac{2A\pi}{3R_A^2 Q^2} \alpha_s(Q^2) x g_N^{\text{DLA}}(x, Q^2)$. We find our result for $F_2^N(x, Q^2)$ to be in excellent agreement with the recent HERA data in the kinematic region of x and Q^2 where DLA is valid⁸.

We parametrize the initial shadowing ratio $R_0^q(x) \equiv F_2^A(x, Q_0^2)/AF_2^N(x, Q_0^2)$ at $Q_0^2 = 0.4$ GeV² using experimental data and we calculate the nuclear structure function at the measured $\langle Q^2 \rangle$ values at different x values. The results for ⁴⁰Ca and ²⁰⁸Pb are shown in Fig. 1.

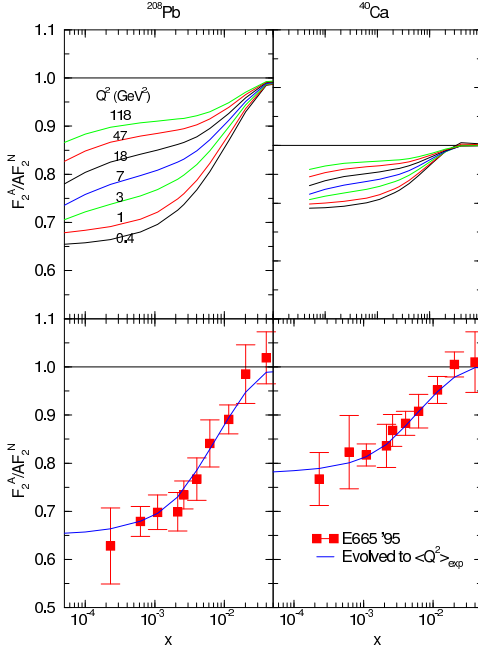


Fig. 1

We note that at large Q^2 the nuclear shadowing effect is reduced but does not diminish, i.e. it is not a higher twist effect. This can be understood as the interplay between the perturbative and the non-perturbative shadowing mechanisms, which is also evident in the x -dependence of R_q ⁸. The apparent flatness of the shadowing ratio at low Q^2 in the small- x region is altered by the perturbative evolution. This is due to the singular behavior of xg_N^{DLA} as $x \rightarrow 0$ at large Q^2 leading to the strong x -dependence of the effective number of scatterings, $\kappa_q(x)$. Furthermore, at small x the Q^2 -evolution of the F_2^A/AF_2^N is much slower than the DGLAP evolution due to multiple scatterings. We illustrate this effect in Fig. 2. When the effective number of scatterings, $\kappa_q(x)$, is small, the Eq. (3) becomes the DLA of the DGLAP evolution equation for quarks.

Similarly, gluon distribution in a nucleus is given by

$$xg_A(x, Q^2) = xg_A(x, Q_0^2) + \frac{2R_A^2}{\pi^2} \int_x^1 \frac{dx'}{x'} \int_{Q_0^2}^{Q^2} dQ'^2 [\gamma + \ln(\kappa_g) + E_1(\kappa_g)] \quad (4)$$

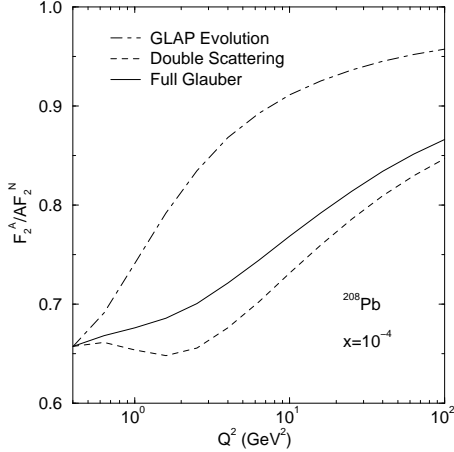


Fig. 2

The essential difference between the quark and gluon cases is different splitting functions and the effective number of scatterings, $\kappa_g = 9\kappa_q/4$ due to different color representations that the quark and the gluon belong to. These two effects combined result in the 12 times faster increase of the gluon density with Q^2 than in the case of the sea quarks in the region of small x . The two important effects which make the gluon shadowing quite different from the quark shadowing are the stronger scaling violation in the semihard scale region and a larger perturbative shadowing effect. This can be seen by considering the shadowing ratio

$$R_g(x, Q^2) = \frac{xg_A(x, Q^2)}{Axg_N(x, Q^2)} = \frac{xg_N(x, Q_0^2)R_g^0(x) + \Delta xg_A(x; Q^2, Q_0^2)}{xg_N(x, Q_0^2) + \Delta xg_N(x; Q^2, Q_0^2)} \quad (5)$$

where $R_g^0(x)$ is the initial shadowing ratio at Q_0^2 and $\Delta xg(x; Q^2, Q_0^2)$ is the change of the gluon distribution as the scale changes from Q_0^2 to Q^2 . The strong scaling violation due to a larger κ_g at small x causes $\Delta xg_N(x; Q^2, Q_0^2) \gg xg_N(x, Q_0^2)$ as Q^2 is greater than $1 \sim 2 \text{ GeV}^2$. As seen in Fig. 3(a) for $Q^2 \geq 3 \text{ GeV}^2$ the dependence of $R_g(x, Q^2)$ on the initial condition $R_g^0(x)$ diminishes and the perturbative shadowing mechanism takes over.

The x -dependence of the gluon shadowing can also be predicted as long as $Q^2 > 3 \text{ GeV}^2$ where the influence of the initial condition is minimal. The

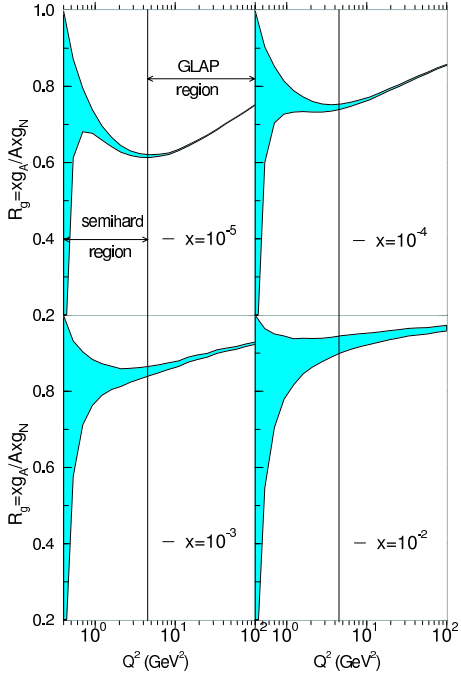


Fig. 3(a)

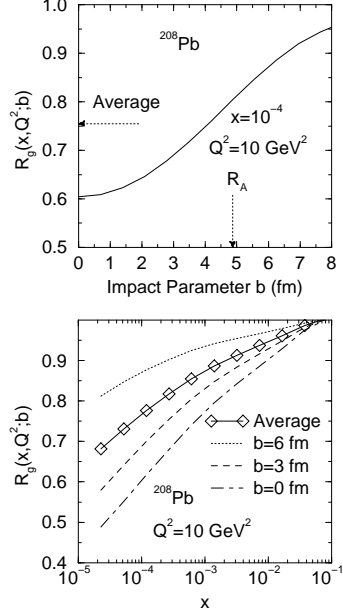


Fig. 3(b)

shape of the distribution is quite robust in the small- x region regardless of what initial conditions one may choose. Due to the perturbative nature of the shadowing, these distributions do not exhibit a saturation as x decreases. Furthermore since the shadowing is a non-linear effect in the effective number of scatterings, the impact parameter dependent shadowing ratio cannot be factorized into a product of an average shadowing ratio and the nuclear thickness function. Our results are presented in Fig. 3(b).

In summary, the nuclear shadowing phenomenon can be understood as a consequence of the parton coherent multiple scatterings. We find that the quark shadowing arises from an interplay between “soft” physics and the semi-hard QCD process. At small x , we find that the quark shadowing ratio evolves with Q^2 slower than the DGLAp evolution. We show that gluon shadowing is largely driven by a perturbative shadowing mechanism due to the strong scaling violation in the small- x region. The gluon shadowing is thus a robust phenomenon at large Q^2 and can be unambiguously predicted by perturba-

tive QCD. The strong scaling violation of the nucleon structure function in the semihard momentum transfer region at small x can be reliably described by perturbative QCD and is a central key to the understanding of the scale dependence of the nuclear shadowing effect. The impact parameter dependence of gluon shadowing is a non-linear effect in the nuclear thickness function. It is important to correctly incorporate the impact parameter dependence of the nuclear structure function when one calculates the QCD processes in the central nuclear collisions. In the asymptotic limit of small x , gluon distribution in nuclei does not exhibit saturation, as in the case of the GLR⁹ equation, but rather tends to the limit $xG_A \sim R_A^2 Q^2 \ln(1/x)$. Thus, the shadowing ratio, R_g , does not saturate at small x , as long as the gluon density in a nucleon has singular x -dependence at small x .

Acknowledgements

The work presented here was done in collaboration with Z. Huang and H.J. Lu. This work was supported in part by the U.S. Department of Energy grants DE-FG03-93ER40792 and DE-FG03-85ER40213.

References

1. NMC Collaboration, P. Amaudruz *et al.*, Z. Phys. **C51**, 387 (1991); Z. Phys. **C53**, 73 (1992); Phys. Lett. **B295**, 195 (1992); NMC Collaboration, M. Arneodo *et al.*, Nucl. Phys. **B441**, 12 (1995).
2. E665 Collaboration, M.R. Adams *et al.*, Phys. Rev. Lett. **68**, 3266 (1992); Phys. Lett. **B287**, 375 (1992); Z. Phys. **C67**, 403 (1995).
3. see e.g., G. Piller, W. Ratzka and W. Weise, Z. Phys. **A352**, 427 (1995); T.H. Bauer, R.D. Spital and D.R. Yennie and F.M. Pipkin, Rev. Mod. Phys. **50**, 261 (1978).
4. S.J. Brodsky and H.J. Lu, Phys. Rev. Lett. **64**, 1342 (1990).
5. R.J. Glauber, in *Lectures in theoretical physics*, ed. W.E. Brittin *et al.* (Interscience Publishers, New York, 1959); R.J. Glauber and G. Matthiae, Nucl. Phys. **B21**, 135 (1970); V.N. Gribov, Sov. Phys. **JETP** 29, 483 (1969).
6. N.N. Nikolaev and B.G. Zakharov, Z. Phys. **C64**, 631 (1994).
7. A.L. Ayala F, M.B. Gay Ducati and E.M. Levin, Nucl. Phys. **B493**, 305 (1997).
8. Z. Huang, H. J. Lu and I. Sarcevic, Nucl. Phys. **A637**, 79 (1998).
9. L.V. Gribov, E.M. Levin and M.G. Ruskin, Phys. Rep. **100**, 1 (1983).